DTIC FILE COPY

AD-A200 080

DTIC ACCESSION NUMBER

PHOTOGRAPH THIS SHEET

LEVEL

INVENTORY 1

AFWAL-TR-88-2088

DOCUMENT IDENTIFICATION

OCT 1988

This document has been approved for public release and sale; its distribution is unlimited.

DISTRIBUTION STATEMENT

ACCESSION FOR	
NTIS	GRA&I
DTIC	TAB
UNANNOUNCED	
JUSTIFICATION	
BY	
DISTRIBUTION /	
AVAILABILITY CODES	
DIST	AVAIL AND/OR SPECIAL
A-1	

DISTRIBUTION STAMP

DTIC COPY INSPECTED

DTIC ELECTE S NOV 01 1988 D E

DATE ACCESSIONED

DATE RETURNED

88 11 01 061

DATE RECEIVED IN DTIC

REGISTERED OR CERTIFIED NO.

PHOTOGRAPH THIS SHEET AND RETURN TO DTIC-DDAC

DTIC FORM 70A DEC 83

DOCUMENT PROCESSING SHEET

PREVIOUS EDITION MAY BE USED UNTIL STOCK IS EXHAUSTED.

AFWAL-TR-88-2088

TIP SENSOR DEVELOPMENT

Lawrence W. Langley

Vatell Corporation
P.O. Box 66
Christiansburg, VA 24073

October 1988

Final Report for Period July 1987 - January 1988

AERO PROPULSION LABORATORY
AIR FORCE WRIGHT AERONAUTICAL LABORATORIES
AIR FORCE SYSTEMS COMMAND
WRIGHT-PATTERSON AIR FORCE BASE, OHIO 45433-6563

REPORT DOCUMENTATION PAGE

Form Approved
OMB No. 0704-0188

1a. REPORT SECURITY CLASSIFICATION UNCLASSIFIED	1b. RESTRICTIVE MARKINGS None
2a. SECURITY CLASSIFICATION AUTHORITY	3. DISTRIBUTION/AVAILABILITY OF REPORT Approved for Public Release; Distribution is Unlimited
2b. DECLASSIFICATION/DOWNGRADING SCHEDULE	
4. PERFORMING ORGANIZATION REPORT NUMBER(S) VTR 88-01	5. MONITORING ORGANIZATION REPORT NUMBER(S) AFWAL-TR-88-2088
6a. NAME OF PERFORMING ORGANIZATION Vatell Corporation 6b. OFFICE SYMBOL (If applicable)	7a. NAME OF MONITORING ORGANIZATION Aero Propulsion Laboratory (AFWAL/POTX) Air Force Wright Aeronautical Laboratories
6c. ADDRESS (City, State, and ZIP Code) P.O. Box 66 Christiansburg, VA 24073	7b. ADDRESS (City, State, and ZIP Code) Wright-Patterson AFB OH 45433-6563
8a. NAME OF FUNDING/SPONSORING ORGANIZATION Aero Propulsion Lab. 8b. OFFICE SYMBOL (If applicable)	9. PROCUREMENT INSTRUMENT IDENTIFICATION NUMBER F33615-87-C-2801
8c. ADDRESS (City, State, and ZIP Code) Air Force Wright Aeronautical Lab. AFSC - United States Air Force Wright-Patterson AFB, OH 45433-6563	10. SOURCE OF FUNDING NUMBERS PROGRAM ELEMENT NO. 65502F; PROJECT NO. 3005; TASK NO. 20; WORK UNIT ACCESSION NO. 86
11. TITLE (Include Security Classification) TIP SENSOR DEVELOPMENT	
12. PERSONAL AUTHOR(S) Lawrence W. Langley	
13a. TYPE OF REPORT Final	13b. TIME COVERED FROM 7/87 TO 1/88
14. DATE OF REPORT (Year, Month, Day) 1988 October	15. PAGE COUNT 44
16. SUPPLEMENTARY NOTATION	

17. COSATI CODES		
FIELD	GROUP	SUB-GROUP

18. SUBJECT TERMS (Continue on reverse if necessary and identify by block number)
Sensor, Clearance, Turbomachine, Blade, Eddy Current

19. ABSTRACT (Continue on reverse if necessary and identify by block number)
Turbomachinery blade clearance and time of arrival sensors based on the Vatell eddy current principle, and suitable for operation at temperatures up to 200 degrees C, were designed, built and tested on the first fan stage of a JT15-D. The sensors produced robust, low noise signals whose general shape is virtually independent of speed, and whose amplitudes are related to speed and clearance. The signals of individual blades were readily resolved and identified. A model equation which predicts sensor signal amplitude, given values of clearance and speed, was developed, and coefficients derived to fit the experimental data. The engine was equipped with an optical once/revolution sensor.

20. DISTRIBUTION/AVAILABILITY OF ABSTRACT ☒ UNCLASSIFIED/UNLIMITED ☐ SAME AS RPT. ☐ DTIC USERS	21. ABSTRACT SECURITY CLASSIFICATION UNCLASSIFIED
22a. NAME OF RESPONSIBLE INDIVIDUAL Christopher J. Worland	22b. TELEPHONE (Include Area Code) (513) 255-6802 22c. OFFICE SYMBOL AFWAL/POTX

DD Form 1473, JUN 86 *Previous editions are obsolete.*

TABLE OF CONTENTS

BACKGROUND INFORMATION

Since about 1969 various experimenters have been exploring the use of casing-based sensors, commonly called "tip sensors", for dynamic measurement of turbine and compressor blade running clearance, deflection and twist. Because casing-based sensors do not require slip rings on the machine shaft, and because they operate in a relatively benign environment, they have the potential of providing lower cost, more reliable blade condition monitoring signals than sensors mounted on the rotating parts of the machine.

Early experimental tip sensors were adapted from commercial electromagnetic proximity detectors. These detectors were installed in turbine housings to sense blade clearance, much as they are used conventionally to detect shaft runout and vibration. The electromagnetic proximity detectors which have been tested and used previously in this application are based on capacitive, magnetic (induction) or eddy current principles. All have been found deficient in one or more respects:

1. Capacitive Proximity Detectors operate by detecting the change in capacitance of a parallel plate capacitor, in which one of the "parallel" plates is the blade, and the other is an electrically isolated element of the detector. The dielectric is the air between the blade and the detector element. The blade is at ground potential, and the detector element is energized by a high frequency, at least an order of magnitude higher than the response frequency desired from the detector. A parallel plate capacitor has a capacitance value that varies with both plate overlap area and distance. The distance between the detector element and the blade (at its closest approach) must be small, in order to have a useful value of capacitance and sufficient variation with blade position for meaningful measurements. The area of the detector plate must be consistent with the precision desired in angular deflection measurement. This constraint typically results in extremely small values of capacitance, of the same order as the capacitance of the wire connecting the detector to its circuit components. Measuring small variations in an initially small value of capacitance with good frequency response is a very challenging instrumentation problem. These detectors are particularly subject to electrical noise pickup, very sensitive to humidity, limited in detection range, and can only be used where runout tolerances and clearances are extremely small.

2. Magnetic, or inductive, proximity sensors derive their signals from the variation of inductance of a coil in the presence of a ferromagnetic object. The inductance variation is measured by driving the coil with a frequency much higher than the sensor response frequency desired. If the blade itself is not ferromagnetic, in order to be detected it must have a target of

ferromagnetic material attached to its end. To obtain good sensor frequency response the gap between the sensor and the ferromagnetic target must also be very small, of the order of.005 inches.

3. Eddy current proximity sensors detect the presence of a conductive blade by measuring the losses of a tuned circuit, one of whose elements is an inductive coil magnetically coupled to the blade. The losses in the coil are influenced by eddy current losses in all conductive objects nearby, including the blade. These sensors can be used with non-magnetic targets (although titanium, a common high strength-to-weight ratio blade material, is a poor target because of its high resistivity) but are severely limited in frequency response. Like capacitive and magnetic sensors their driving frequency must be an order of magnitude higher than the desired response frequency. The more sensitive the tuned circuit is to eddy current losses in the blade, the higher its "Q", and the longer it will take to respond to a change. The frequency response of eddy current sensors is generally more limited than that of capacitive or inductive sensors. However, they are more tolerant of environmental conditions than the capacitive or inductive types.

4. Weigand wire sensors employ a magnetic switching phenomenon in a wire combining permanent and soft magnetic materials, to produce voltage impulses in response to an externally applied magnetic field. This type of sensor requires that a permanent magnet target be applied to each blade, and can only be used to signal blade time of arrival. Weigand wire sensors were tested by Shaker Research Corporation (1), who found that the timing of sensor impulses was too random and unpredictable for the intended use.

Other tip sensing schemes which are in use or on test in turbomachines are servo-positioned spark-gap probes, and optical sensors of various types. The spark-gap probe can only measure the clearance of the longest blade in a machine, so its primarily application is in calibrating other tip sensors. Optical probes, however, have been tested as clearance sensors and as time of arrival sensors since about 1976.

NASA Lewis sponsored extensive studies of optical tip sensors by Shaker Research Corporation (1),(2),(3) in 1980 and 1981, and there have been testing programs at Pratt and Whitney (4) and Brown Boveri & Cie (5). These programs have explored the use of optical sensors along with techniques for processing sensor data to derive blade deflection, twist, and clearance data from it. While these investigations have demonstrated that optical sensors have the sensitivity and bandwidth needed for useful measurements, they have not shown that such sensors can meet long-term machine monitoring requirements. In fact, the consensus seems to be that contamination is a severe problem for

optical sensors in the turbomachinery environment, requiring purging or other measures to maintain a clear optical path.

Tip sensor signal processing to derive measurements of blade clearance, deflection and twist has been the subject of extensive research at Virginia Polytechnic Institute (6). There is a large amount of information in tip sensor signals which may be valuable for machine monitoring and control, if the information is found to be precise enough and can be extracted in real time at reasonable expense. VPI research indicates that the signal processing needed for a functional tip sensor turbine monitoring system is technically and economically feasible. However, existing sensors have lacked the capability to transduce blade proximity with sufficient bandwidth, accuracy and long term reliability.

In 1986 Vatell Corporation developed a tip sensor which employs a new eddy-current principle for producing clearance and blade time-of arrival signals. Prototypes were tested in 1987 on a Pratt & Whitney (Canada) JT15-D jet engine at VPI, under private sponsorship. These tests indicated that an important capability for jet engine monitoring and control could possibly be developed from the new sensor concept.

SENSOR PRINCIPLES OF OPERATION

Figure 1 is a schematic view of the Vatell sensor, which illustrates its principles of operation. The sensor contains two magnets, a flux bridge and a coil, all within a housing which is filled with an encapsulant. The sensor is shown in a typical orientation relative to a moving turbomachine blade made of electrically conductive material such as titanium.

One of the two magnets (1) is oriented with its North pole adjacent to a flux bridge. The second magnet (2) is oriented with its South pole adjacent to the flux bridge. The combination of the two magnets and the flux bridge produces a static magnetic field in the region traversed by the blade, adjacent to and between the South pole of magnet (1) and the North pole of magnet (2). The shape of this field and its extent are as described by Herbert C. Roters in Chapter 5 of his textbook "Electromagnetic Devices", published by Wiley. Figures 6a and 6b of the reference are particularly illustrative of the lines of force and the equipotential lines of the field of such a magnet. In the absence of any moving conductive objects in the region between the open poles of the two magnets, the field will not vary with time. Thus the field surrounding the coil will be constant, and no voltage will be produced at the terminals of the sensor.

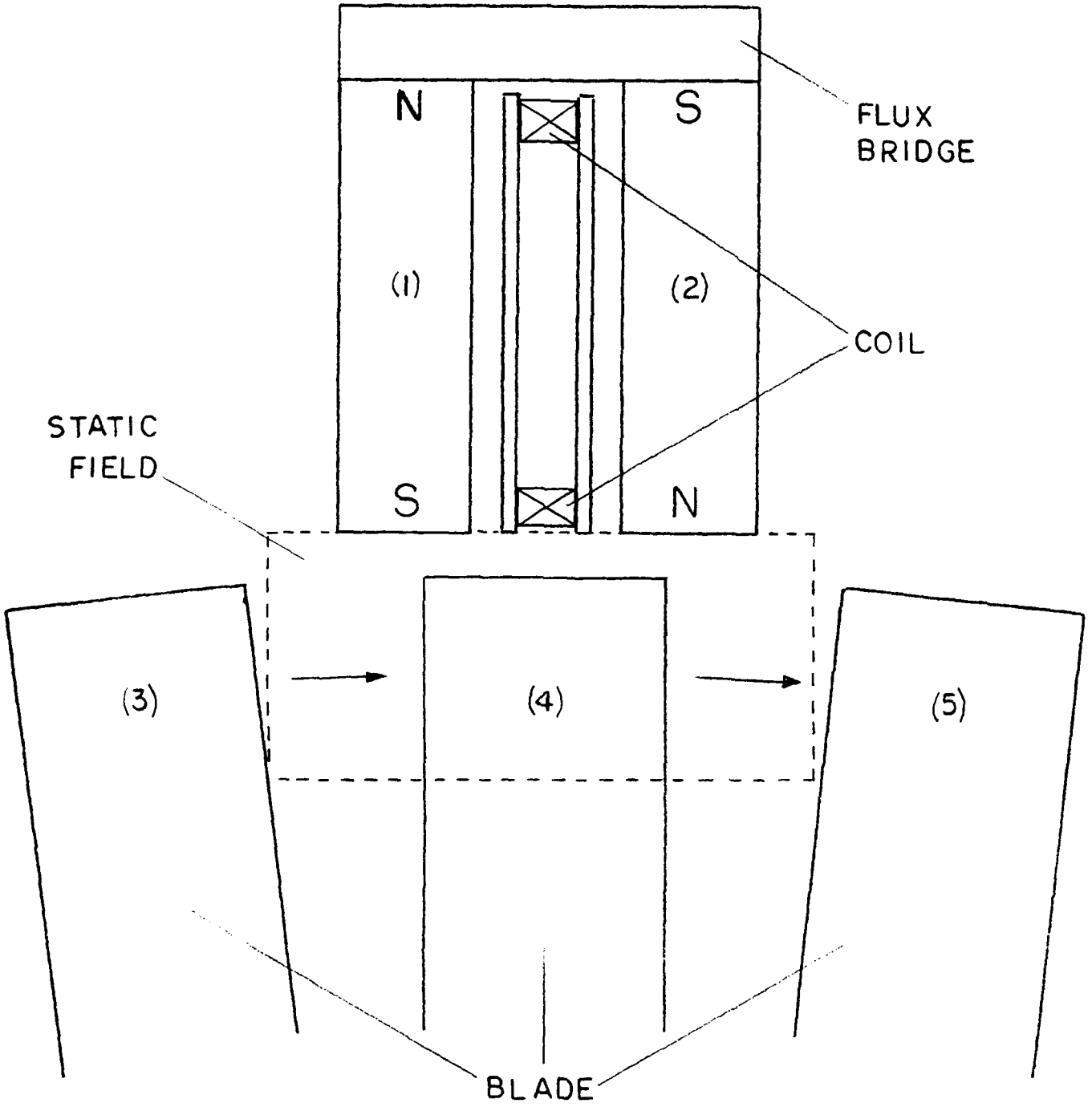

FIG. 1

The effect of the blade on the static magnetic field, and the voltage produced by its motion in the coil, are best understood by visualizing that the blade is initially in a position (3), moving toward and through the position (4) to the position (5). As the blade begins to intercept field lines of the magnet, eddy currents will be induced in the conductive material of the blade. These currents will flow in the blade in a pattern and direction which oppose the increase in flux density passing through the blade material. The currents will effectively induce a magnetic field within the blade which is equal and opposite to that of the permanent magnet. External to the blade this field is constructively attached to the blade, and its motion relative to the coil will induce a voltage in the turns of the coil. This voltage is initially positive with the coil intercepting an increasing proportion of the eddy-current field. When the blade reaches the centered position (4) the eddy currents in the blade quickly reverse direction, because the field of the permanent magnet intercepted by the blade stops increasing and starts to decrease. The rapid reversal of eddy currents causes a rapid reversal of the induced field polarity seen by the coil, and a large negative peak voltage is produced because the field produced by these currents is closely coupled to the coil at this position. As the blade moves away from the centered position, the field intercepted by the nearest turns of the coil then decreases, and a second positive voltage peak is produced. It is positive because the polarity of the eddy currents has reversed and the blade is now moving away. The characteristic "Schmoo" shape of the signal is the result of the growth and decay of eddy currents in the blade and the change in their coupling to the coil.

Eddy currents in the moving blade are produced by the motion of the blade through the permanent magnet field, and their amplitude is thus proportional to the velocity of the blade. The voltages induced in the coil are also produced by relative motion, and are proportional to the blade velocity as well. The combination of these two proportionalities yields a square-law relationship between the signal level and the speed of the blade. The shape of the signal does not change with speed because the resistivity of the blade material is low and the eddy currents are dissipated only slightly by resistive losses. The inductance of the coil has a minimal effect because currents are induced in it by changes in the external field, rather than by voltages imposed on its terminals. The signal is therefore an almost pure indication of mechanical position because its frequency content is far removed from the decay time constant of eddy currents on the low side and from the detection circuit's time constants on the high side.

The coupling of the permanent magnetic field to the blade, and the coupling of the coil to eddy-current induced transient fields, are both affected by the angle between the blade chord

and the axis of the coil. For maximum signal, the plane of the sensor, which is the same as the plane of the coil, should be parallel to the blade chord. This orientation yields a maximum coupling between the permanent magnet and the blade material, and a maximum coupling between the coil and the eddy currents in the blade.

Coupling between the magnetic field and coil of the sensor and the blade material is also affected by the distance from blade to sensor. As the gap between them is increased, the signal induced by eddy currents will diminish. Thus the signal amplitude may be used for the measurement of blade clearance, if the effects of blade velocity can be compensated for. Key questions are, how consistent is the velocity effect, and is the signal sufficiently free of noise to make it a precise indicator of blade clearance? These are questions addressed by the present contract.

TECHNICAL OBJECTIVES

The sensors which Vatell built and tested earlier under private sponsorship were designed for room temperature operation. They were constructed for a quick series of tests, and were not expected to survive long term use. They were tested with readily available instrumentation which had neither the bandwidth nor the storage capacity to fully characterize the sensor signal. The engine was not equipped with a "once-per-revolution" sensor, which would be necessary to identify individual blades and compare successive signals from the same blade. An objective of the present contract was to correct these deficiencies. Prototype sensors were to be produced and tested under conditions which would allow confident prediction of their characteristics in potential applications.

WORK PLAN

The first stage of work was to build new sensors suitable for long term use at up to 200 degrees centigrade. High temperature magnet material, wire, insulation system, and encapsulation epoxy were substituted for the materials used in the earlier units. The new design took into account the thermal expansion and other effects of exposure to a high temperature operating environment. The new sensor design is one which houses the permanent magnet, winding and all connections within a Titanium shell. The shell is filled with an epoxy resin for maximum environmental protection and reliability.

The second stage of work was to test the prototype sensors on the JT15-D engine at VPI, using equipment and test methods which were improved over those of earlier privately sponsored tests. Certain hardware which was used in earlier tests could be used

again. However, in these tests the engine was equipped with a once/revolution sensor which allowed identification of the signal from each individual blade. Data was recorded using a high-speed digital oscilloscope with a precision of 12 bits, time resolution of 0.5 microsecond and memory for 4,096 samples. With this equipment it was possible to compare clearance and arrival time for individual blades over a variety of operating conditions.

The third stage of work was to characterize the relationships between signal amplitude, tip clearance and speed for the new sensor. A mathematical model for sensor voltage output as a function of clearance and speed was developed, and its empirical constants filled in with experimental values.

Each of the three stages is described in detail in the sections following.

SENSOR DESIGN

The objectives of the sensor redesign were to achieve:

* 200°C continuous rating
* Improved sensitivity
* Closed-end metallic housing
* Encapsulation for reliability and durability

Figure 2 illustrates the new sensor design, which met all these objectives. The housing was fabricated from 3/8 inch OD, .019 wall thickness 3.5V 2.5Al Titanium alloy tubing. A rim was swaged on the open end of the housing for locating the sensor axially.

The permanent magnets in the sensor are Incor 24HE, a 2:17 Samarium Cobalt alloy which has the lowest temperature coefficient of remanence of any rare earth, and a service temperature well above 200°C. The operating point for the magnets is high enough so that they do not need to be keepered.

The sensor wire is Thermalex 200, AWG #46, rated at 220°C. It is wound on a bobbin of Ultem 1000-1000, which has a continuous service temperature of 180°C, but will survive 200°C with reduced strength.

The sensor lead wire is Brim Electronics No. 1791 shielded twisted pair AWG 24 (19 strands #36) with both conductors and shield insulated by Teflon. It is rated at 200°C continuous. Solder is 60/40, with a melting point of 227°C.

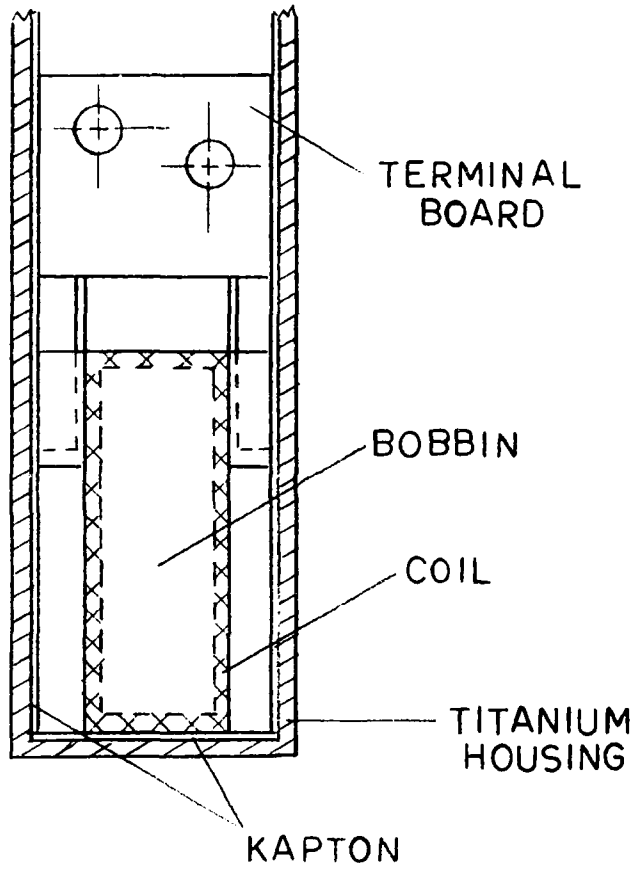

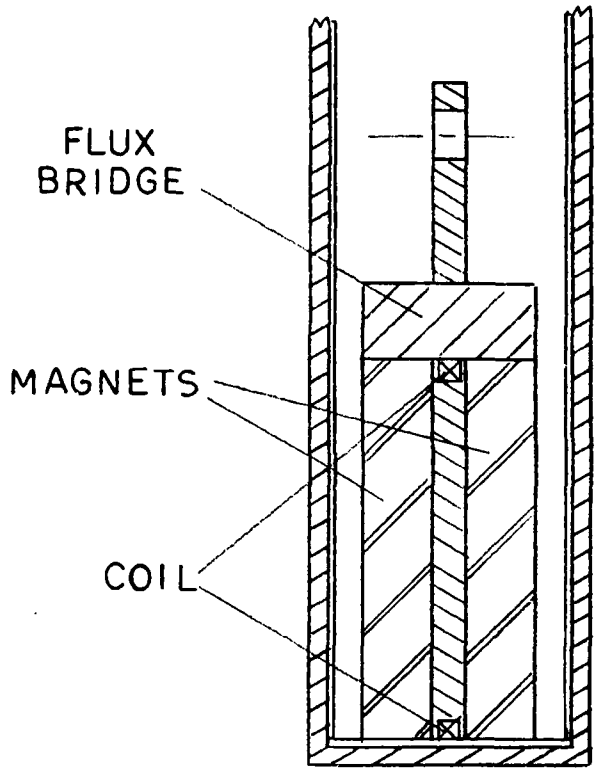

VATELL CORPORATION

CLEARANCE SENSOR

SCALE 4:1

FIG. 2

The encapsulation system is Emerson & Cuming 2850FT resin cured with Catalyst 17 in 3 temperature steps, rated at 220°C continuous. The end and sides of the magnet-coil assembly are isolated from the housing by a .004" film of Kapton, which is rated at 220°C.

SENSOR DESIGN PROCESS

During this project many alternatives were explored in the choice of materials and in the sensor configuration. In this section the most important of these alternatives, and the rationale for the final choices, will be described.

Tubing

Initially there was a serious concern that the metallic closed end of the housing would attenuate the signals produced by blade eddy currents. The original project plan was to fabricate closed-end sensors using the highest resistivity metal available, and subject them to preliminary tests. If their measured signal level was too low, the ends of these sensors would be ground off in small steps until an acceptable signal level was achieved. This proved to be unnecessary, but there was no way to predict this at the outset.

Metals reference books indicated that Titanium alloys would have the best combination of resistivity and high temperature performance as a sensor housing material. Alloy 8-1-1 (8% Aluminum, 1% Molybdenum and 1% Vanadium) was selected for its resistivity range of 54 to 150 μ-ohm-cm. This material could not be found in the form of tubing, however, so it was purchased in sheets, with the intention of rolling and welding closed-end tubes. No vendor could be found who would guarantee both an inside and outside diameter concentricity of tubes welded from this material, however. It appeared that a compromise would have to be made on alloy resistivity.

The most readily available Titanium tubing is aircraft hydraulic line, usually made of alloy 3.5V/2.5Al (3.5% Vanadium, 2.5% Aluminum). No information could be found on the resistivity of this alloy, but it was said to be reasonably malleable. The first approach was to cut blanks from this tubing and weld ends of alloy 8-1-1 onto them. After considerable discussion of this idea with an experienced Titanium fabricator, it was decided instead that closed-end tubes would be fabricated from 3/8" O.D., .019" wall tubing by a swaging-welding-forming process. In this process the tubing end is swaged to a roughly rounded end, welded shut, then formed over a mandrel to final dimensions. This process could be tooled to produce a dimensionally consistent part, but the prototypes would be made on "jiffy" tooling and would not be so precise.

Magnets

The principal concern in selection of the magnet material was the change in sensor sensitivity which would result from the variation of remanence (B_r) with temperature. To achieve maximum sensitivity for the sensor a high B_r material is desired, and the highest values for rare earth magnets are found in Neodymium-Iron alloys. Unfortunately these magnets have relatively high temperature coefficients of remanence (typically 0.11%/°C) and maximum operating temperatures below 200°C. The material finally selected, Incor 24HE, has a temperature coefficient of 0.025%/°C, which yields a predicted sensitivity variation of 5% or less over the temperature range 0 to 200°C. The maximum operating temperature for Incor 24HE is 350°C and B_r at 200°C is 9.6 Kilogauss.

A possible second concern about the magnets used in the sensor would be their operating point. The ratio of magnet area (in a plane normal to the direction of magnetization) to magnet length (in the direction of magnetization) determines the open circuit permeance coefficient, a measure of the operating point. At low values of permeance coefficient the magnets experience less demagnetization, and are more stable with temperature. The design of the Vatell sensor is such that a long, slender magnet, operating at a low permeance coefficient, is required anyway, in order to make room for the coil which detects eddy currents.

Wire

The selection of wire was straightforward and posed no design difficulties. The wire size of AWG #46 allowed the number of turns to be increased over earlier sensors by a factor of 5. Instead of two separate coils wound around the magnet poles, a single coil of 100 turns was wound on a bobbin, then placed between the magnet poles. AWG #46 is very small wire (.0016" diam.), but no difficulties were experienced in winding it or in making the connections to the sensor lead wires. Coil resistance turned out to be 42 ohms.

Encapsulation

There are relatively few encapsulation systems which will survive long exposure to a temperature of 200°C. Stycast 2850FT, manufactured by the Emerson & Cuming Division of W. R. Grace & Co., is commonly used in electric motor and electronics manufacturing to protect fine windings from mechanical damage at high temperatures, and was felt to be a good choice for this application. When cured with Catalyst 17, this filled resin is rated for long term exposure to 220°C. Stycast 2850FT has a relatively high viscosity, however, and problems were anticipated in getting a good fill of the housing. At room temperature the resin has a consistency about like that of molasses (viscosity =

85,000 cps @ 25°C). The only strategy available was to carry out epoxy mixing and pouring at the highest possible temperature, in this case the manufacturer recommended 80°C. At this temperature the mix begins to cure and set up quickly, so time was of the essence in mixing and filling. Housings were held for filling in large blocks of refractory brick preheated to 80°C. All components of the mix were preheated, as were all containers and implements. After an end insulator and sleeve of Kapton were placed in the housing, epoxy was dispensed by syringe; about 50% of the amount required to encapsulate each sensor was pre-filled before inserting the magnet\coil assembly; the remainder was post-filled. Housings were then placed in a curing fixture with their closed ends against a surface of soft iron. Attraction of the sensor magnets to the iron pulled the magnet coil assembly firmly to the bottom of the housing tube, displacing the epoxy resin and insuring that the magnets were tightly held against the inside of the end cap insulator during the curing process.

Lead Wire

Since the output of the sensor is balanced and isolated from ground, the best possible immunity to noise is achieved by using a shielded, twisted pair cable for connection to the differential amplifier. Cable with all teflon insulation was selected to meet the 200°C temperature requirement. It was decided that the titanium shell would not be grounded to this cable because the electrical potential of the engine was unknown, and currents through the shield would be likely to produce more noise than that which might be picked up electrostatically by the coil and its connections within the sensor. Since the cable termination and all parts of the sensor (including magnets) were isolated from the housing by .004" of Kapton and the encapsulation as well, it was believed that an adequate breakdown voltage between shield and housing would be achieved. Connections between the conductors of the cable and the #46 wire of the sensor coil were made at terminals mounted on a small circuit board of Ultem 1000-1000.

SENSOR FABRICATION

The process of building sensors was straightforward, though time-consuming and requiring a good deal of patience. Using a Coweco LA-3 coil winder, bobbins were wound with 100 turns each of #46 wire in about 1.6 hours each. The terminals were staked onto their terminal boards, then bobbins, magnets, back iron and terminal boards were aligned and tacked together with an anaerobic adhesive. A total of five units were assembled to this level in about 5 more hours. Several bobbins were broken during this stage of assembly. The ends of the #46 wire were chemically stripped and soldered to the terminals, then the lead wires soldered to the opposite ends of the terminals, in another 5

hours. Pieces of Kapton to fit the inner ends of the housings, and rectangular pieces to wrap around the assemblies inside the housings, were prepared, and inserted into the housings, taking about 1 hour.

Three sensors (Units #1, #2, and #3) were encapsulated in a first batch. The difficulty of filling a narrow tube with a viscous epoxy became quite evident. The magnet-bobbin assemblies were inserted into their respective titanium tubes, and it was then discovered that it was quite impossible to pour the epoxy in a narrow enough stream to have it flow into the housing around the lead wires. The assemblies were then removed and the epoxy was partly poured, partly ladled in until the housings were about half full, then the assemblies were inserted again. This method succeeded, but there was still quite a bit of difficulty in "topping up" the housings with epoxy. The first three sensors were then given a single temperature cure to harden the epoxy, without attempting to achieve ultimate high temperature performance.

A second batch of sensors (Units #4, #5) was assembled after conferring with the epoxy resin manufacturer on pouring techniques. His recommendation was to raise the temperature of every component used in mixing and pouring to 80°C. This would reduce the pot life to less than a half hour, but at least the mix would be initially less viscous. He also recommended use of a syringe for dispensing the mixed epoxy.

Special fixtures were made to increase thermal inertias, and everything was soaked in the oven at 80°C for four hours before starting. This time it was a great deal easier to dispense the epoxy into the housings, although they were still partially pre-filled before the assemblies were inserted. The purpose of this was to make sure that the ends were completely sealed, in case it became necessary to grind off the end caps to increase the signal level. This batch of sensors was given a three temperature step cure to maximize high temperature performance. After the cure they were checked for continuity and grounds, and the magnet orientation was marked by using a "Magnet Visualizer," a liquid crystal device which responds to magnetic field lines by producing light and dark patterns.

TEST PREPARATIONS

The most important improvement in the test apparatus also turned out to be the most difficult to achieve. In earlier privately sponsored tests there was no way to match signals with individual blades, so analysis of the relationship between amplitude vs. speed and clearance had to be based on averages. In this contract a once/revolution sensor was to be added to the JT-15D engine so that each blade signal could be uniquely identified in

the recordings. There were a number of constraints to be taken into account, however.

1. Any mass added to the rotor would have to be small enough not to unbalance it.
2. There were two penetrations available on the engine housing, one adjacent to the compressor blade ends, 1/2 inch in diameter, and one in line with the base of the hub, with a diameter of 15/16 inch.
3. Any sensor which penetrated the engine housing would have to be flush with its inner surface, and designed so it could not shed parts into the compressor under any circumstances.
4. The once/revolution sensor should have sufficient bandwidth to produce a sharp signal clearly identifying an index position, and time repeatability of a few microseconds or less.

Fiber Optic Sensor

A modulated infrared beam fiber optic sensor designed for high speed motor commutation was borrowed from Inland Motor in Radford, VA. and installed in the penetration next to the N1 compressor. This sensor had been designed for use with black and white shaft marks. High contrast paints which had been used successfully by Inland in developing motor commutation signals were used to mark the ends of compressor blades; one with a white mark and the rest with black. Tests were run at low engine speeds, and two problems were encountered. The duration of the signal produced by the white paint was so short that the sensor did not see it, and the paint rapidly lost its contrast as the engine ran. Problems were encountered with noise pickup; the output of the sensor was a fraction of a volt, making it difficult to use in the engine test environment. This approach was abandoned.

Modulated Infrared Scanner

The next sensor tested was a Microswitch FE7B RA6G-M subminiature diffuse scan photoelectric. This unit uses a modulated infrared beam to distinguish between dark and light colored surfaces at distances up to 6 inches. It has a separate LED light source and phototransistor receiver, housed side by side. The frequency rating of the FE7B is 15,000 operations/minute, sufficient for a rotor speed of 15,000 rpm. This is not the maximum speed of the JT-15D, but would be adequate for these tests. Scanning the hub from the second penetration, its distance from the target would be about 7 inches, depending on the details of mounting. It was felt that with high contrast paints and the excellent dimensional control of the engine application, this sensor would have a chance of working.

A mounting bracket and window were designed for the FE7B. The window, made of Lexan, was tested to prove that it could not be pulled into the compressor under the most adverse circumstances. A force of 3000# was applied to a sample window without a failure. The sensor was then mounted on the engine and the hub was painted with a stripe of white paint. At low speeds a good signal was obtained, but the sensor bandwidth was insufficient to produce a signal at full speed. The hub was then painted 50:50 with black and white paint. At full speed the signal was adequate, but another problem was encountered. The modulation frequency of the scanner, about 100 Khz, produced an uncertainty in timing of more than a blade interval at full speed. While this might be acceptable for sensor tests, it would be confusing, and would not work at all in an automatic blade identification system. It was decided to look for a scanner with an unmodulated light source.

Retroreflective Scanner

The next scanner tested was a Microswitch FE-R3T1 retroreflective unit with incandescent light source. This scanner is designed for use with reflective codes at a fixed distance of 6 inches, and has a design bandwidth of about 15,000 Hz. The scanner is normally sold with a control base which supplies 5.5 volts to the incandescent lamp and amplifies the phototransistor signal to operate a relay or logic output. To give maximum operating flexibility, a SOLA 81-05-230-1 limited range adjustable voltage power supply was purchased instead of the control base, so that lamp excitation could be varied if desired.

A new mounting was designed for the R3T1, and it was installed on the engine. A signal of a fraction of a volt could be derived from the black and white paint, but this was not adequate to serve as a reliable once/revolution indication. At this point it began to appear that nothing was going to work. A retroreflective target supplied with the scanner produced a strong signal, but there was no way to mount it on the hub without creating a severe unbalance, and the 50% light/dark duty cycle requirement could not be met. A retroreflective tape also produced a strong signal, and could be applied to 50% of the hub circumference, but there was serious doubt whether it would stay in place at full engine speed, and many concerns about what would happen if the tape were ingested into the engine.

The final solution was to apply a retroreflective paint, 3M Scotchlite product 7216, to the hub, leaving 50% of the circumference unpainted. The resulting signal was stable and of sufficient amplitude to serve as a once\revolution indication. Figure 3 is an oscillogram of this signal. From the lowest speed of the engine to the highest there was less than a blade pitch variation in the location of this signal, so it could be used not only in experiments, but in a future automatic blade

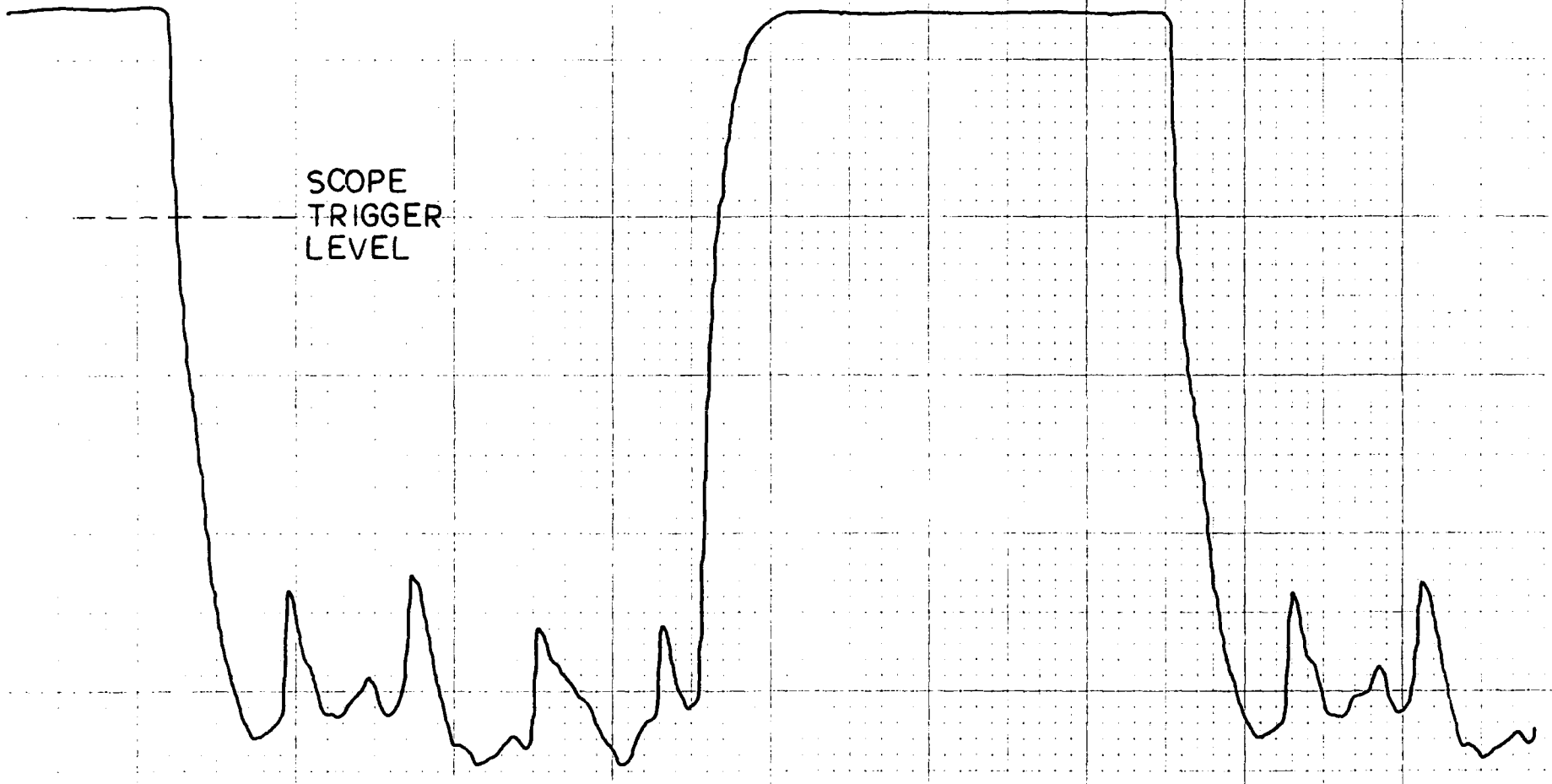

FIG. 3

identification system, as well. The figure shows amplitude variations along the bottom of the waveform caused by the heads of fasteners on the hub, which reduce the reflected light beam slightly. The triggering level for the oscilloscope was set well above these to avoid sporadic triggering.

Data Acquisition System

It was determined that the sensor clearance traversing stage used in earlier tests would be adequate, and the Dynamics 7521B amplifier used earlier would also work. A Nicolet 2090 Digital Oscilloscope with type 206 plug-in and a floppy disk storage unit was obtained for data recording. This oscilloscope will sample two channels at 2 Mhz per channel, converting two analog signals to 12 bit digital data. Its storage capacity is 4096 samples per record, whether taken from one channel or two. Eight records of 4096 samples each can be recorded on a single-sided floppy disk, then played back later for display, analysis or conversion to graphical hard copy. Once data is taken with this instrument it can be examined at leisure, because the absolute values of timing and amplitude are recorded for every sample point, and do not lose accuracy with repeated playback. A Mosely 7030A X-Y recorder from Hewlett-Packard was used to produce graphical outputs.

SENSOR TESTS

The first test was a simple run with sensor #1 to determine whether it worked at all, if so what the waveforms looked like, and to get a rough idea of signal amplitudes. These tests revealed that the signals were essentially the same in shape as those of earlier sensors, but their level was much greater than expected; up to 60 millivolts peak-to-peak. Furthermore, the noise was more than 60 db. below the peak signals. All thoughts of having to grind away the sensor ends were given up as unnecessary. Data acquisition equipment was acquired and assembled for actual tests.

The second series of tests on the engine also used sensor #1 from the first batch. In these tests the sensor was clamped in the traversing stage with its end flush with the inner surface of the housing, and with the stage on zero. The sensor axis was aligned with the blade chord within about 5°. The once/revolution signal was connected to channel A of the oscilloscope, the sensor signal to channel B. A gain of 50 was selected on the Dynamics amplifier.

With the engine operating at idle, some difficulty was experienced in triggering the oscilloscope on the once/revolution signal. This was found to be caused by the dc offset of the signal: if sufficient gain was used to produce a trace with the

amplitude required for triggering, the signal was off-scale. This was corrected by using the (-) differential input of the oscilloscope, subtracting the power supply voltage from channel A. The result was steady and reliable triggering by channel A, with settings which did not have to be adjusted at all during succeeding tests.

Waveforms were recorded at each of five speeds for the N1 spool, nominally 5000, 7000, 10,000, 12,000 and 14,000 rpm. The engine speed was then reduced to idle, and the test cell was opened up and entered to adjust the clearance. This was done by withdrawing the sensor into the engine housing on the micrometer stage. The clearance was set at .005, .010, .015 and .020 inches away from the zero position, and traces were made for all five speeds at each setting. Some traces were recorded several times at different gain settings and sample rates. 64 records were captured on disk for later analysis.

Figure 4 shows the waveforms for the once/revolution sensor superimposed on the clearance sensor waveform. The clearance sensor waveforms are not accurately represented here because of resolution limitations of the plotter and a plotting algorithm in the oscilloscope which blends data points together. A more detailed and precise view of the Blade 0 waveform is shown in Figure 5. This shows the data which the Nicolet oscilloscope provides on each feature of the sensor output. The amplitudes are direct sensor output voltages, and times are relative to the oscilloscope trigger point. From the times it can be determined that the waveform for Blade 0 is roughly centered on the fall time of the once-per-revolution sensor signal. Figure 6 shows the waveforms for Blades 0 and 1, illustrating the separation between blades achieved by this sensor. Speed has <u>essentially no effect</u> on this separation. Figure 7 shows slightly less than 1/4 of a revolution of the rotor; a typical record from which signal amplitudes and speed may be determined accurately.

It was observed during the second series of tests that the heights of waveforms for individual blades were extremely consistent. Blade numbers could be determined easily from an inspection of the blade waveforms alone, because of their characteristic amplitude pattern. The only unusual variations in blade timing or amplitude were observed at a speed of about 8,000 rpm, where a persistent engine vibration had been noted earlier. The test cell operating instructions had been modified to not allow a dwell at that speed for any amount of time. Because of this limitation, detailed observations were not made at this speed. It is not known whether engine vibration caused the sensor movement relative to the rotor, or if the blades themselves were vibrating at this speed.

Data from Run #2 was plotted and appeared to be regular. However, it was noted that in a cross-plot of signal amplitude

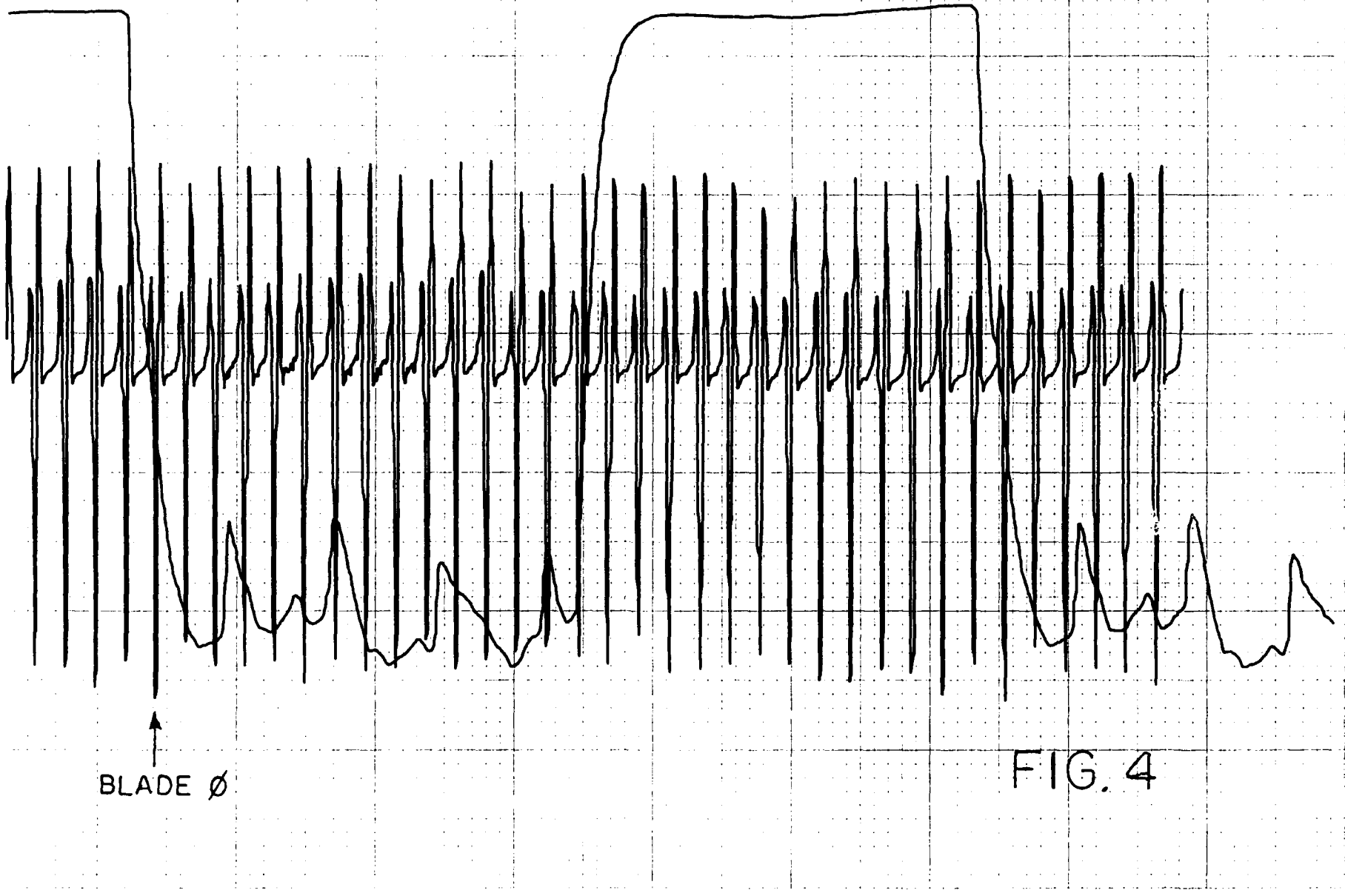

FIG. 4

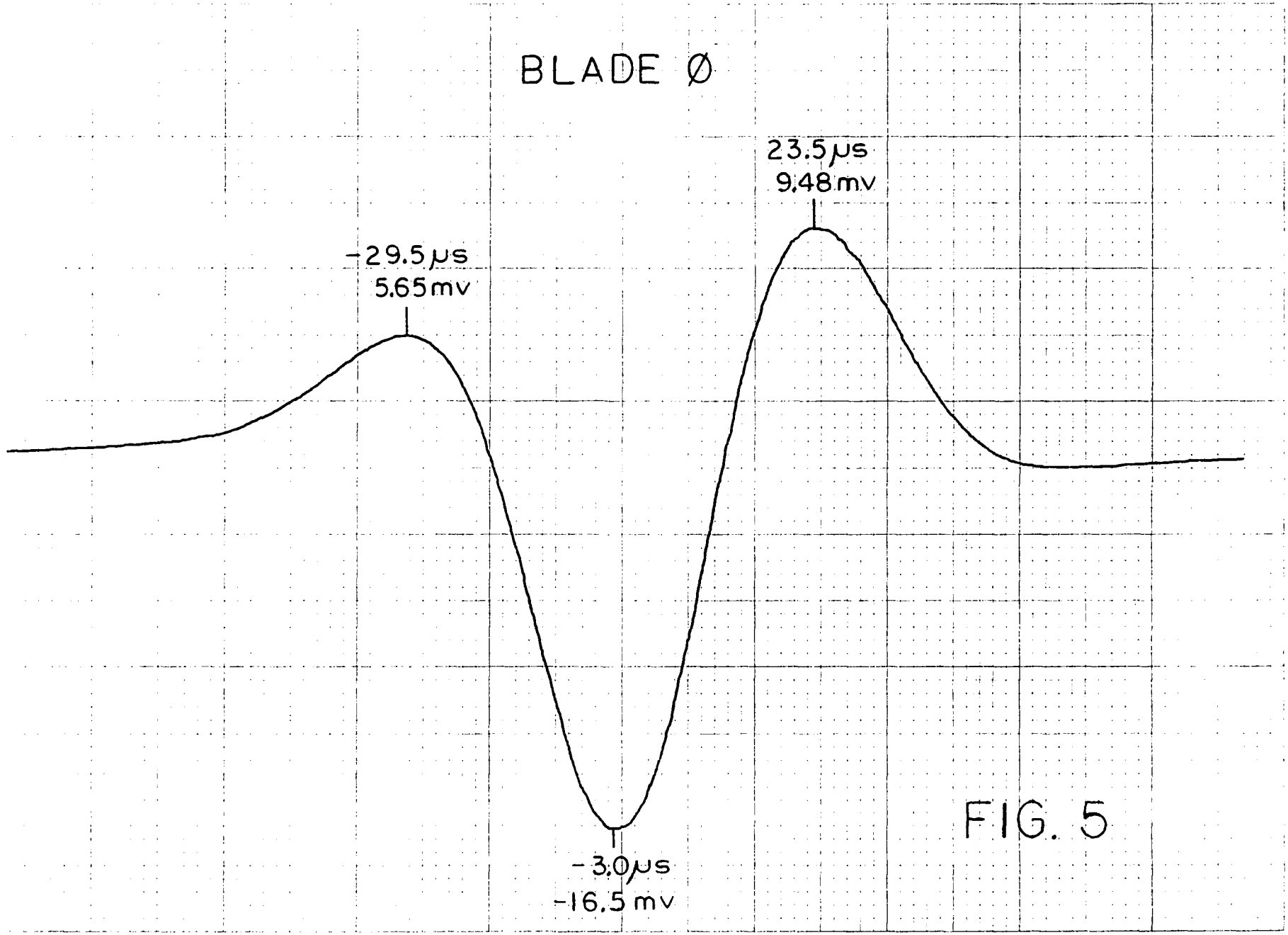

FIG. 5

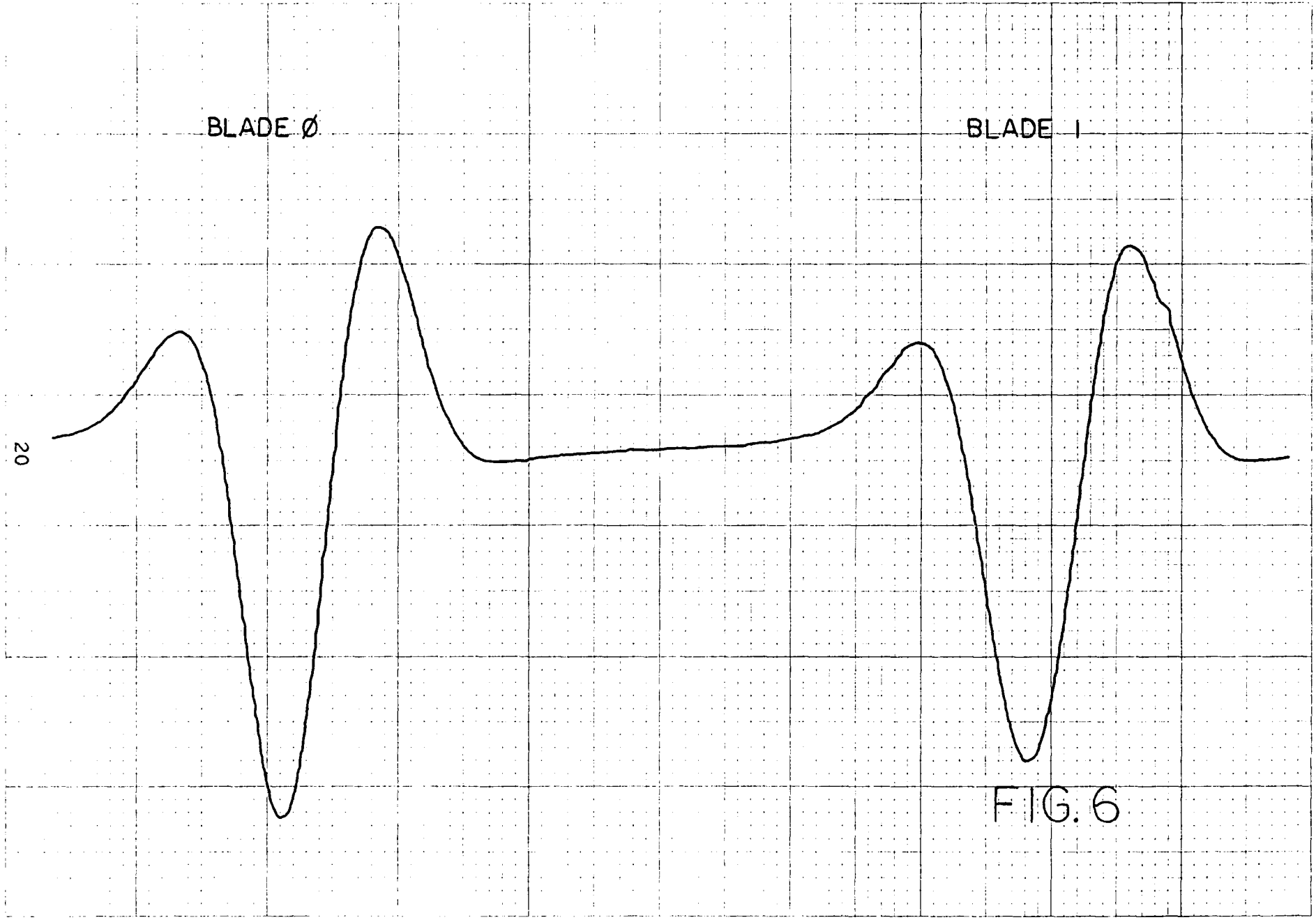

FIG. 6

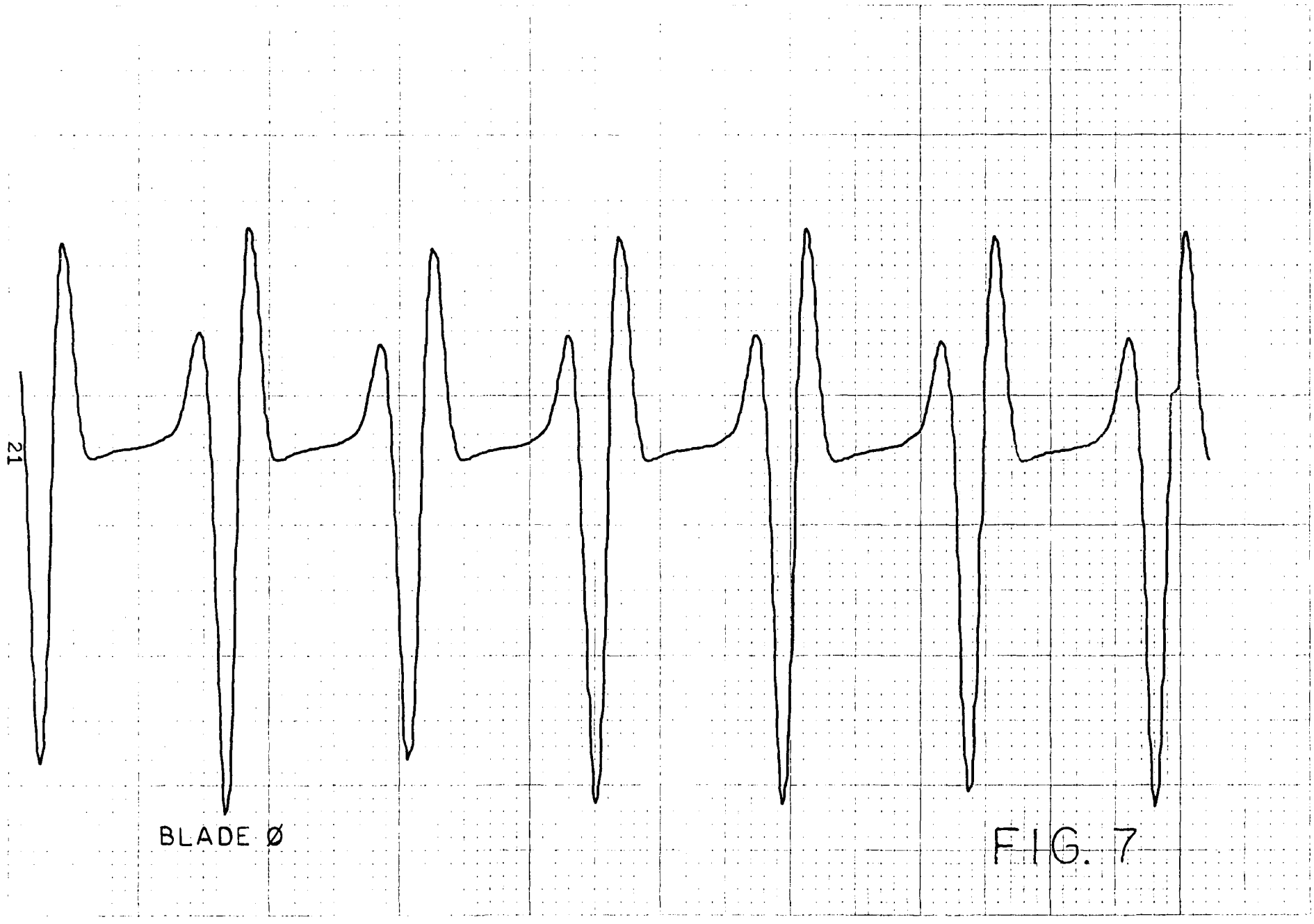

FIG. 7

vs. clearance, holding speed constant, the points for .020 displacement did not line up with the others. The micrometer stage in the test cell was re-examined, and it was found that the last clearance setting had actually been .019". Even after adjusting for this error, the scatter of the data appeared excessive, so it was decided to run another series.

The third series of tests on the engine was with Sensor #4 from the second encapsulation batch. In this series only one record was made for each speed and clearance combination, but more speeds and clearance values were tested. A total of 70 records were made at 7 speed values and 10 clearance values. Again the data was regular in appearance.

ANALYSIS OF THE DATA

Data taken in Runs 2 and 3 are listed in Tables 1 and 2, and plotted in Figures 8 and 9, respectively. Data points are interconnected with straight lines in the plots only to make them easy to associate with their curves. In all cases the amplitude of the Blade 0 signal is represented on the Y axis, and in all cases but one the speed along the X axis was calculated from the times of the most negative points of peaks from Blades 27 and 6. This is equal to 1/4 of a revolution. Record 2-8 (Disk #2, track #8) did not contain 7 full signals, so the speed calculation for this record used the timing of peaks from Blades 27 and 5.

TABLE 1

Tabulation of Data from Run #2
Sensor #1 Blade 0 Signal

Record No.	Displacement	RPM	Amplitude (mv)
1-2	.000	4759	3.89
1-5	.000	7389	10.46
1-8	.000	10,623	25.98
2-2	.000	12,361	39.88
2-3	.000	14,340	61.88
2-6	.005	4747	3.22
2-8	.005	7252	8.94
3-3	.005	10,145	20.09
3-7	.005	12,019	32.07
4-2	.005	14,104	50.76
4-3	.010	4717	2.80
4-7	.010	7386	8.15
5-2	.010	9934	16.80
5-4	.010	11,552	25.47
5-6	.010	14,198	44.44
5-8	.015	4739	2.45
6-3	.015	7253	6.55
6-6	.015	10,115	15.38
6-8	.015	12,082	24.69
7-2	.015	13,902	36.14
7-4	.019	4723	2.17
7-7	.019	7102	5.73
8-2	.019	10,302	14.16
8-4	.019	11,928	22.10
8-6	.019	14,238	35.70

TABLE 2 - 1

Tabulation of Data from Run #3
Sensor #4 Blade 0 Signal

Record No.	Displacement	RPM	Amplitude (mv)
9-1	.000	4667	3.65
9-2	.000	5952	5.91
9-3	.000	8170	12.72
9-4	.000	9416	18.25
9-5	.000	11,013	27.47
9-6	.000	14,327	56.48
9-7	.000	12,658	41.02
9-8	.000	10,424	23.48
10-1	.001	4867	3.68
10-2	.001	6117	6.24
10-3	.001	7772	10.45
10-4	.001	9410	17.38
10-5	.001	11,029	27.45
10-6	.001	12,809	41.24
10-7	.001	14,111	53.22
11-1	.002	4726	3.32
11-3	.002	7882	10.99
11-4	.002	9554	17.96
11-5	.002	11,136	26.58
11-6	.002	12,542	36.94
11-7	.002	14,098	52.02
12-1	.003	4723	3.26
12-2	.003	6471	6.60
12-3	.003	8161	11.86
12-4	.003	9609	17.43
12-5	.003	11,177	26.13
12-6	.003	12,626	36.52
12-7	.003	14,191	51.46
13-1	.004	4832	3.37
13-2	.004	6297	6.16
13-3	.004	7945	10.98
13-4	.004	9696	17.45
13-5	.004	11,304	27.15
13-6	.004	12,658	36.38
13-7	.004	14,071	47.36

TABLE 2 - 2

Tabulation of Data from Run #3 (continued)
Sensor #4 Blade 0 Signal

Record No.	Displacement	RPM	Amplitude (mv)
14-1	.005	4759	3.17
14-2	.005	6505	6.24
14-3	.005	7945	10.49
14-4	.005	9740	17.03
14-5	.005	10,949	23.44
14-6	.005	12,637	34.22
14-7	.005	14,058	47.42
15-1	.010	4744	2.64
15-2	.010	6567	5.66
15-3	.010	7886	8.81
15-4	.010	9560	14.32
15-5	.010	11,095	20.51
15-6	.010	12,766	31.14
15-7	.010	14,164	40.48
16-1	.015	4667	2.20
16-2	.015	6460	4.68
16-3	.015	7962	7.72
16-4	.015	9524	11.97
16-5	.015	11,086	17.95
16-6	.015	12,605	25.04
16-7	.015	14,151	35.53
17-1	.020	4735	1.95
17-3	.020	7962	6.83
17-4	.020	9579	10.32
17-5	.020	11,321	16.73
17-6	.020	12,864	23.45
17-7	.020	14,151	31.31
18-1	.025	4729	1.67
18-2	.025	6405	3.32
18-3	.025	8134	5.92
18-4	.025	9574	8.86
18-5	.025	11,186	13.82
18-6	.025	12,637	18.88
18-7	.025	14,272	26.67

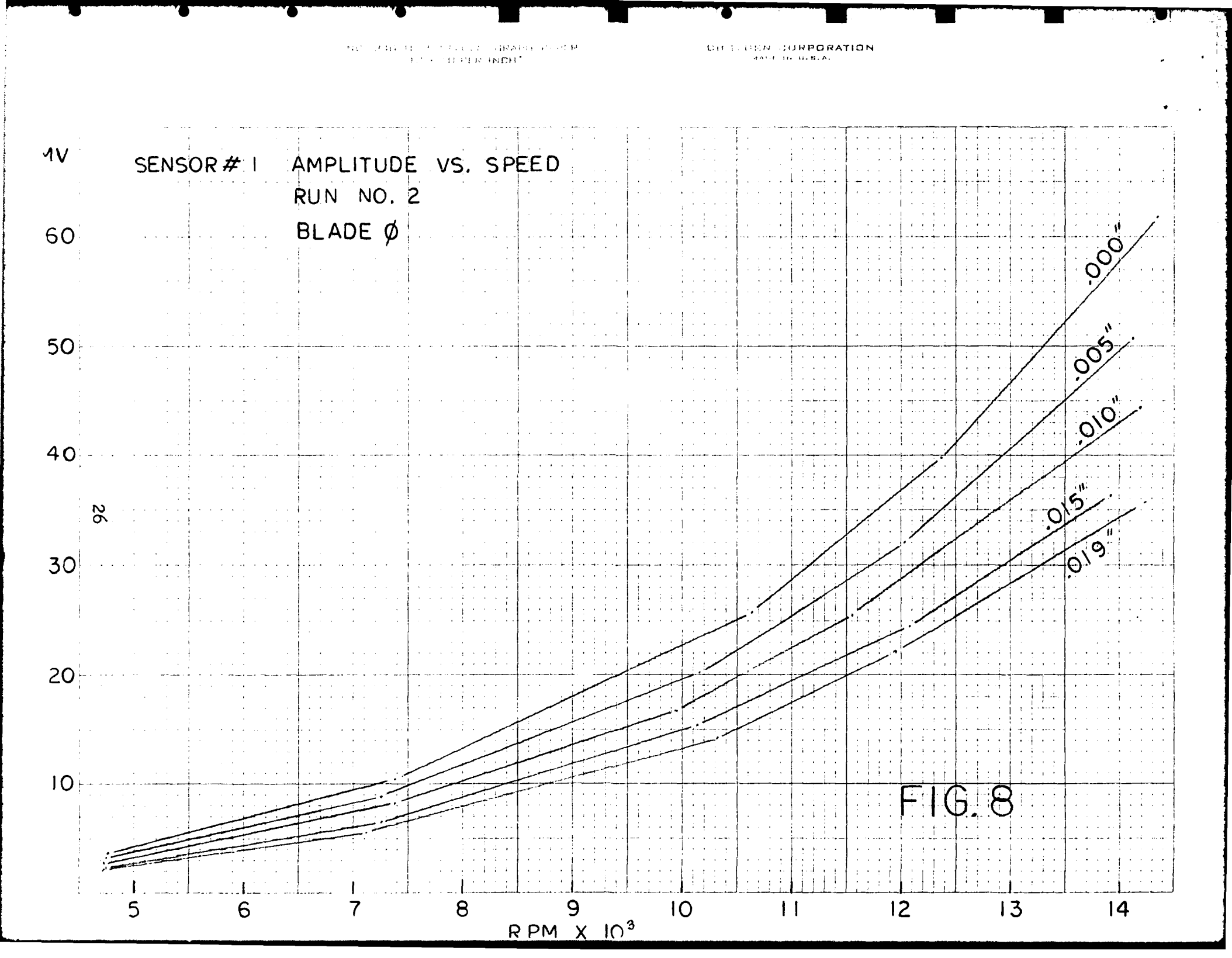
SENSOR # 1 AMPLITUDE VS. SPEED
RUN NO. 2
BLADE Ø
MV
60
50
40
30
20
10
26
.000"
.005"
.010"
.015"
.019"
5
6
7
8
9
10
11
12
13
14
RPM X 10³

FIG. 8

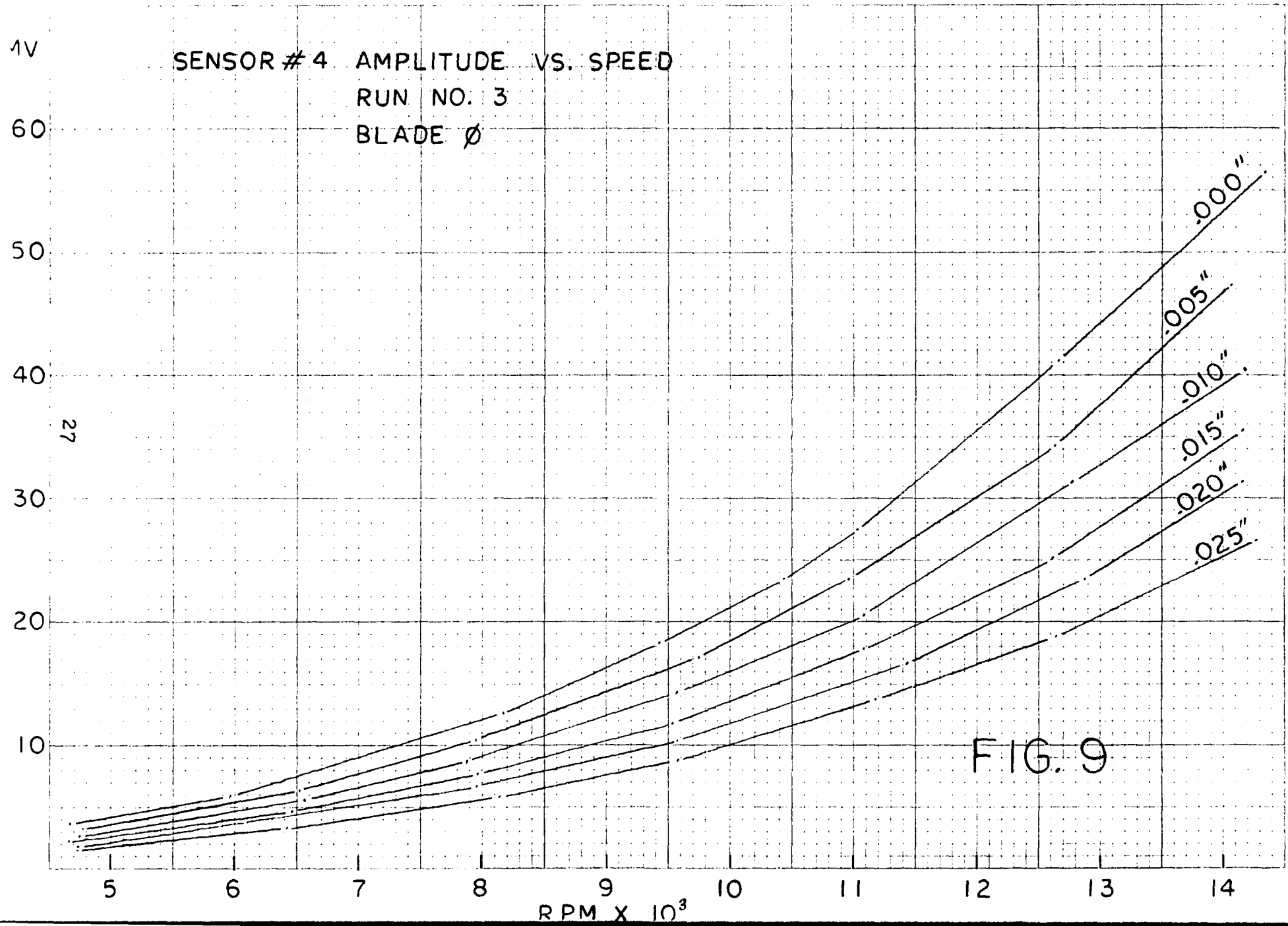

FIG. 9

The analysis was started by trying to determine the general shape of the curves of amplitude vs. displacement for each speed. Because the electromagnetic mechanism which generates the signals in this sensor is not well understood, there is a basic philosophical problem involved in selecting the form of the equation to which the data will be matched. Once an equation form has been selected, deriving the coefficients may be considered a "trivial" task. The rationale followed in selecting the equation form was as follows:

(1) It is believed that eddy currents in the blade will increase in proportion to speed, because the rate at which the fixed permanent magnet field strength must be opposed to exclude flux from the blade will be proportional to speed.

(2) The voltage produced in a coil by a given level of field strength is proportional to the velocity of relative motion. Thus the signal amplitude should have a component proportional to speed squared, and the general form of the equation will be a quadratic.

(3) Fitting a general quadratic equation to the data, the resulting values for the constant term and the multiplier for speed were examined to determine how important they are to the final value, and to try to ascribe a "meaning" to them.

Either an exponential or a quadratic would fit the data equally well. However, there seems to be no rationale for using an exponential function, so a quadratic of the form $AX^2 + BX + C$ was fitted to the data for each individual displacement for Run No. 2, using a least-squares criterion for the best fit. The coefficients of the best fit equations came out as follow:

Displacement	A	B	C
.000	5.88×10^{-7}	-5.30×10^{-3}	16.3
.005	4.76×10^{-7}	-3.99×10^{-3}	11.8
.010	3.89×10^{-7}	-3.01×10^{-3}	8.56
.015	3.29×10^{-7}	-2.50×10^{-3}	7.02
.019	3.29×10^{-7}	-2.75×10^{-3}	8.08

The magnitude of B and C and the sign of B were surprising. The physical meaning of these terms can only be speculated upon. The B term may represent a shielding effect of the engine housing, which is certain to have eddy currents generated in it by the moving field of the blade. Since displacement of the blade is simulated in these tests by withdrawing the sensor into the housing, one would expect this coefficient to increase with displacement, but it does not. The meaning of the C term has not been explained.

These coefficients were examined to determine whether there was any obvious relationship between the curves for different sensor displacements. Cross-plotting the data using the best-fit quadratics revealed an interesting possibility, shown in Figure 10. It appeared as though the curves might be best represented by a family of hyperbolas. It was decided to use non-linear regression methods to model an equation of the form:

$$\text{Amplitude(mv.)} = \frac{AS^2 + BS + C}{D + Y}$$

Where

S = Speed in RPM
Y = Displacement - In.

Data from runs 2 and 3 were used individually because the relationship between the sensor "0" positions was unknown. The coefficients determined for the two runs were as follow:

Constant	Run 2 (Sensor 1)	Run 3 (Sensor 4)
A	1.03×10^{-8}	9.67×10^{-9}
B	-4.89×10^{-5}	-6.18×10^{-5}
C	0.075	0.159
D	0.0245	0.0220

The values for the constant D were particularly interesting because of a possible physical interpretation of their meaning. The expression (D + Y) might be considered to represent the <u>total physical distance</u> from the actual blade tip to the end of the sensor. With this interpretation, the signal amplitude would tend to increase without limit as the clearance between the sensor and the blade tip approaches zero. In these tests the static clearance between the tip of Blade 0 and the physical end of the sensor was about .030 Inches. Actual running clearance could not be measured, but is probably slightly less.

Following up on the idea that the coefficient B might represent a shielding effect, and that this would be proportional to gap, an equation of the form:

$$AS^2 + BS + C(S + Y) + DY + E$$

Where Y is the displacement in inches

was fitted to the data for runs 2 and 3 combined. The resulting coefficients were:

A	3.995×10^{-7}
B	-2.261×10^{-3}
C	-.1147
D	586.7
E	4.605

This equation seems to fit the data better than the simple

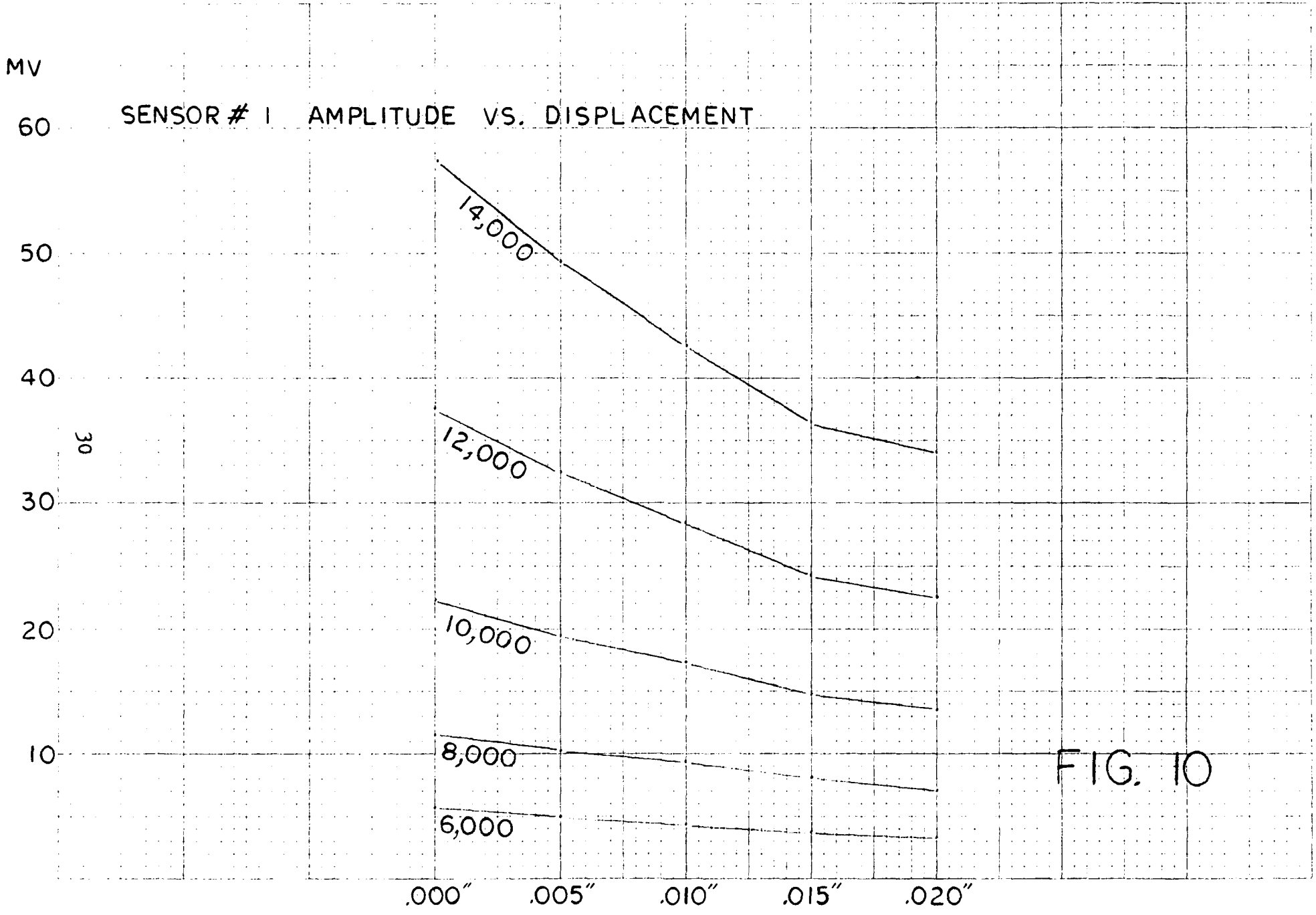

FIG. 10

quadratic, but the values predicted outside the experimental ranges of speed and displacement do not make any sense at all. Furthermore, one cannot readily extract the variable Y in order to compute blade clearance when the amplitude and timing are known. This is a fatal flaw, because the ultimate application for the sensor requires such a computation. The "best fit" expression is therefore regarded as a statistical oddity of no practical value. Despite its deficiencies, the quadratic relationship appears to be the best model.

What are the sources of error in the measurements made on this sensor, and in what manner are they likely to have influenced the data? To determine what the accuracy limits of the sensor signal might be in measuring gap or blade timing, the noise level was measured. The level of noise does not vary with engine speed or sensor gap, and is about 17 microvolts peak-to-peak, as shown in Figure 11, a blow-up of the interval between the signals of Blades 27 and 0 at 4729 RPM and a displacement of .025 Inches. The actual peak-to-peak value of the signal was 1.67 millivolts, (the lowest signal recorded during the entire test) so the noise was 40 db. below this.

The errors in measuring signal timing and amplitude were reduced by employing accurate instruments, by making all amplitude measurements on the same blade tip, and by using the same 1/4 revolution of the machine for all timing measurements. A number of uncertainties and possible sources of error still remain, however.

(1) While the mounting of the sensor to the engine housing is reasonably rigid, the housing and rotor can move relative to each other. At certain speeds a cyclic variation in the sensor signal levels was observed which would indicate that such relative motion was occurring. However, the amplitude of this motion could not be measured.

(2) The "home" position of the sensor relative to the housing was established by different methods and different operators on the two runs, so there is no way to tell what the absolute values were. The micrometer slide position could be adjusted to within ±.0001", and was not affected visibly by vibration. All adjustments were made in one direction to reduce the effects of mechanical lash, and the engine was running in all cases.

(3) Mechanical growth of the blade as machine speed increased could not be taken into account. Close inspection of the experimental data would seem to indicate that the physical length of the blade is increasing with speed, but there was no attempt to distinguish this effect from the general difficulty of fitting the data to the equations. Evidence of blade growth might be a cubical or higher order

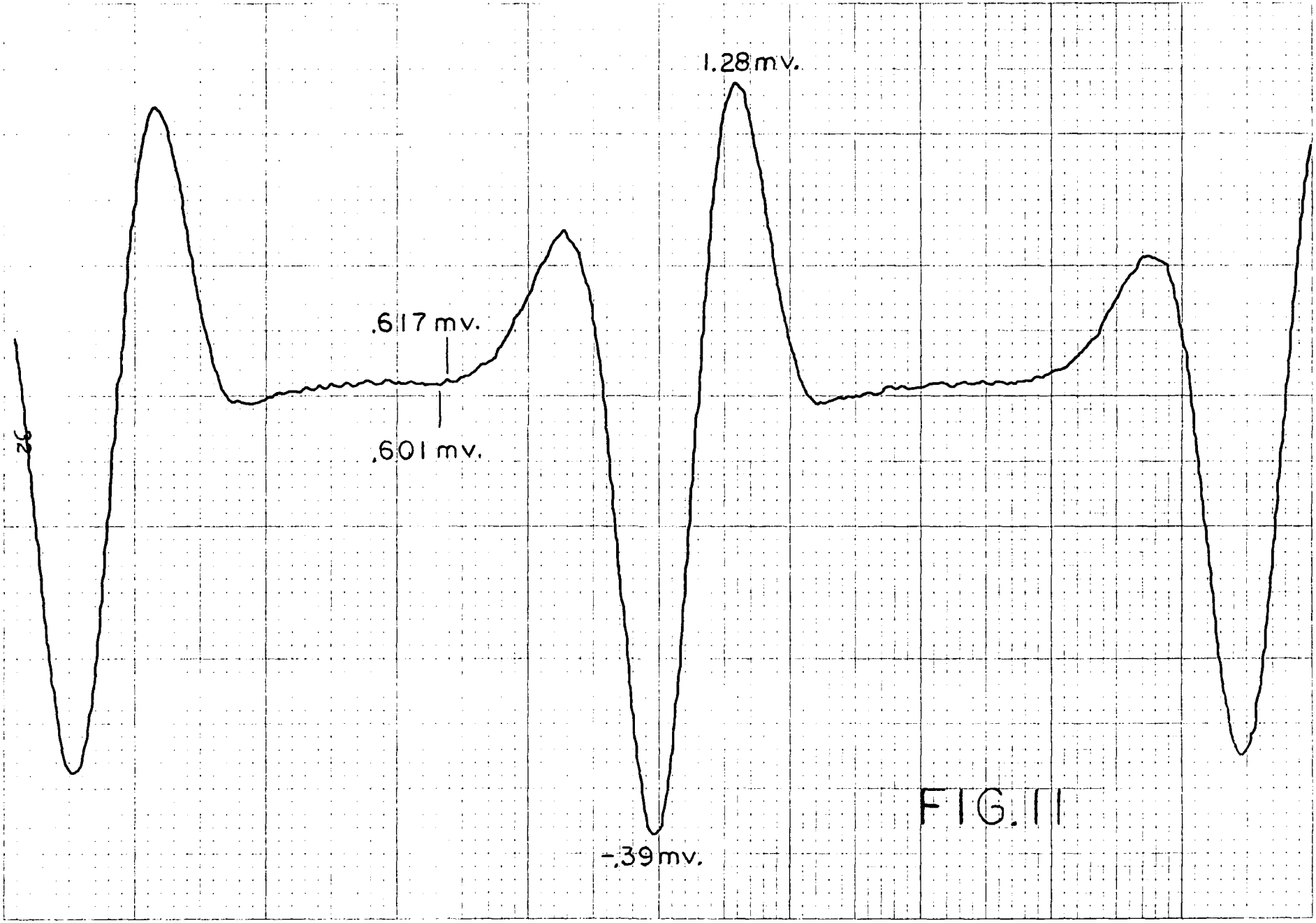

FIG. 11

relationship between amplitude and speed, but it might or might not be mathematically regular.

(4) Blade vibration had unknown effects. Both timing and amplitude measurements might have been affected by blade vibration, and the relationship between measured machine speed, signal amplitude and sensor displacement could have been disturbed. This was not evaluated.

While the absolute accuracy of this sensor in measuring clearance has not been demonstrated, its precision can be estimated by regarding the peak-to-peak noise as the primary uncertainty in amplitude measurement, and converting this to an equivalent clearance value. At the "home position" of the sensor, a nominal clearance from Blade 0 of .030, the estimated precision is ±.00001" at 14,000 rpm, or ±.0001" at 6,000 rpm. Because the "gain" of the sensor is a function of speed, its greatest precision is at the highest speed.

Differences between the measured signal levels of this sensor and signal levels which simple equations would predict can no longer be regarded as evidence that the sensor is inaccurate. The sensor signals are so low in noise, and exhibit such consistency and fine detail that they are bound to represent physical reality in a useful fashion. While this program has helped achieve an understanding of the relationship between this sensor's signal amplitude, speed and displacement, some challenging tasks remain.

CONCLUSIONS

Turbomachinery blade clearance and time of arrival sensors based on the Vatell eddy current principle, and suitable for operation at temperatures up to 200°C were designed, built and tested. The sensors produced robust, low noise signals whose general shape is virtually independent of speed, and whose amplitudes are related to speed and clearance in a regular manner. The signals of individual blades were readily resolved and identified. Timing measurements with an accuracy of 0.5 microsecond and amplitude measurements accurate to 1 part in 4000 can be made with these sensors with reliable, consistent results.

In the analysis of the data, it was assumed that the sensor signal amplitude would be a function of speed squared. Based on this assumption, coefficients for a general quadratic were determined for the signals at fixed displacements. The coefficient for variation of signal proportional to speed was surprisingly large, and negative. It is believed that this is the result of eddy currents in the engine housing. Examination of the data yielded the conclusion that the sensor signals can be modeled by an equation of the form:

$$\text{Amplitude(mv.)} = \frac{AS^2 + BS + C}{D + Y}$$

Where

S = Speed in RPM

Y = Displacement - In.

Coefficients were determined for two sensors in separate runs, and the results invite interpretation of the quantity (D + Y) as the total distance from sensor end to blade tip. This is a potential means of calibration for the sensor. Without another measure of actual tip clearance for comparison, there is no way to evaluate this as a possibility.

FUTURE RESEARCH

The electromagnetic interactions which produce the signal in the Vatell sensor are not well understood. There are no analytical models for eddy currents produced by motion of conductive objects through a static magnetic field. Finite element magnetic modeling techniques are presently inadequate for analysis of this problem, but hold the greatest hope of an ultimate solution. An improved understanding of the signals of this sensor would result from a program to model its electromagnetics using finite element techniques. Further experiments to characterize the sensor's operating characteristics may be suggested by such an analysis.

The operating principle of this new sensor will allow its use at temperatures up to approximately 1000 degrees Fahrenheit.

Judging by expressions of interest from turbomachine manufacturers, a clearance sensor which can operate for a long time at this temperature would be extremely valuable and useful. A program to develop and test such sensors will involve the use of ceramic materials and high temperature magnets, assembled in a design which will survive transient and long term exposure to the full operating range of engine conditions. Testing such sensors will involve modifications to a turbine, an entirely different matter from installing a probe next to a fan. It is believed that a high temperature clearance sensor would require temperature compensation, and reference measurements of clearance might have to be obtained for calibration purposes.

Sensors and signal processing circuitry capable of timing measurements with a precision of better than a microsecond would be very useful in blade vibration research and monitoring. To date only optical sensors have achieved this level of precision: they are apparently unsuitable for long term monitoring. With attention to shielding and minimization of spurious signals, the Vatell sensor could probably meet this requirement. Extremely high speed processing of the signals would then be required, utilizing advanced DSP chips and methods.

In a companion SBIR proposal, Vatell offers to develop high speed signal processing for the signals produced by this sensor. There are many opportunities, not all explored in the referenced proposal, for study and experiment leading to new and useful turbomachine operating test equipment and methods.

REFERENCES

(1) Wilson, D. S., "An Investigation of Sensors Suitable for Monitoring Blade Deflections for a VA1310 Wind Tunnel Compressor" - AFWAL-TR-81-3076 Final Report on Contract F33615-79-C-3019 July 1981

(2) Kiraly, L. J., "Digital System for Dynamic Turbine Engine Blade Displacements" - Measurement Methods on Rotating Components of Turbomachinery, ASME Gas Turbine Symposium, New York, 1980

(3) Wilson, D. S., "Compressor Blade Monitoring System for a VA1310 (Allis Chalmers) Wind Tunnel Compressor" - Final Report AFWAL Contract No. F33615-79-C-3019 July 1980

(4) Barranger, J. P. and Ford, M. J., "Laser Optical Blade Tip Clearance Measurement System" - Measurement Methods on Rotating Components of Turbomachinery, ASME Gas Turbine Symposium, New York, 1980

(5) Roth, H. "Vibration and Clearance Measurements on Rotating Blades Usin Stationary Probes" - Measurement Techniques in

Turbomachines, Von Karman Institute For Fluid Dynamics Lecture Series, May 18-22, 1981

(6) O'Brien, W. F., Sparks, J. F. and Dellinger, D. F., "Non-Contacting Method for Measurement of Dynamic Blade Motions in Axial-Flow Compressors" - Proceedings of the 27th International Instrumentation Symposium, ISA, Indianapolis, IN, April 1981

FE7B Subminiature diffuse scan controls

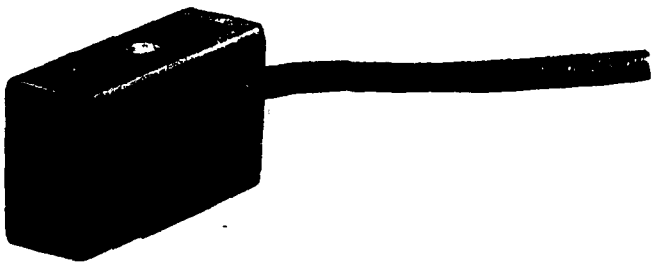

FEATURES

- 6-inch diffuse scan range
- 10 to 28 VDC operation
- Sealing: NEMA 12 and IP64
- Modulated infrared LED for ambient light rejection
- *Combination alignment/self diagnostic indicator*
- *Sensitivity adjustment*
- *False pulse and reverse polarity protection*
- *Short circuit protection*
- *Synchronous detection*
- *Vertical or horizontal mounting choice*

ORDER GUIDE

Description	Listing
Light operated (L.O.) sinking (NPN) output; horizontal mount	FE7B-DA6-M
Light operated (L.O.) sourcing (PNP) output; horizontal mount	FE7B-DD6-M
Dark operated (D.O.) sinking (NPN) output; horizontal mount	FE7B-DB6-M
Dark operated (D.O.) sinking (NPN) output; vertical mount	FE7B-DA6V-M

INSTALLATION/WIRING

Instruction sheet PK 9074 is included with each control, and is also available upon request.

Standard Relay Or Solenoid
Sinking Output

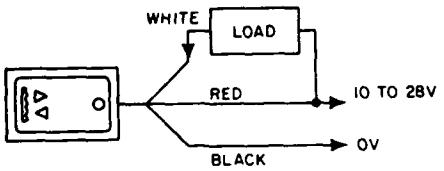

Sourcing Output

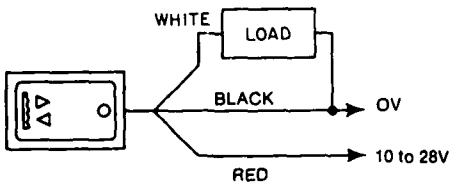

Solid State Circuit

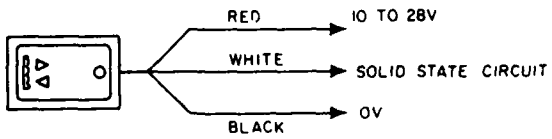

GENERAL INFORMATION

The small package size of FE7B diffuse scan controls allow usage in limited access and/or restricted space areas. A mounting bracket (included) makes mounting and alignment easy. Each control is self-contained, incorporating a pulsed LED, phototransistor receiver and amplifier circuitry with solid state output in one package. The FE7B operates on a broad range DC voltage from 10 to 28 VDC and provides current output up to 100 mA.

FE7B diffuse scan controls incorporate a self diagnostic function alignment indicator. When a sufficient light level is being received, the indicator light is green. But when the light level decreases to 150% of the minimum operating level the indicator turns red. This simplifies installation, alignment, and troubleshooting. A sensitivity adjustment is a standard feature.

FOR A COMPLETE CONTROL

Required

- Diffuse scan control — FE7B-DA6-M
- Appropriately rated DC power supply

Optional

- Retroreflective scan control — See FE7B retroreflective scan controls
- Thru scan control — See FE7B thru scan controls
- Control base

SPECIFICATIONS

Maximum Scanning Distance (in clean air)		6 inches (15 cm)
Supply Voltage		10 to 28 VDC; 10% max. power supply ripple
Power Dissipation		0.56 watts max. (excluding load)
Current Consumption		20 mA max. (excluding load)
Output	Load Current	100 mA max. (open collector, light or dark operated)
	Voltage Drop	1.0 VDC max. sinking 100 mA
	Leakage Current (Off state)	—
Maximum Rate of Operation		15,000 operations/minute
Typical Response Time	On	2 msec.
	Off	2 msec.
Circuit Protection		False pulsing, Short circuit, Reverse polarity
Temperature Range		–4°F to 140°F (–20°C to 60°C)
Sealing		NEMA 12 and IP64
Housing		Case ABS resin, Lens PMMA resin, Cable vinyl
Mounting		Horizontal or vertical side mounting bracket included
Weight		3.5 ozs. (99,2 g)
Logic		Built-in ON-OFF (immediate response) control; light or dark operated by individual catalog listing

MOUNTING DIMENSIONS

Horizontal Mount

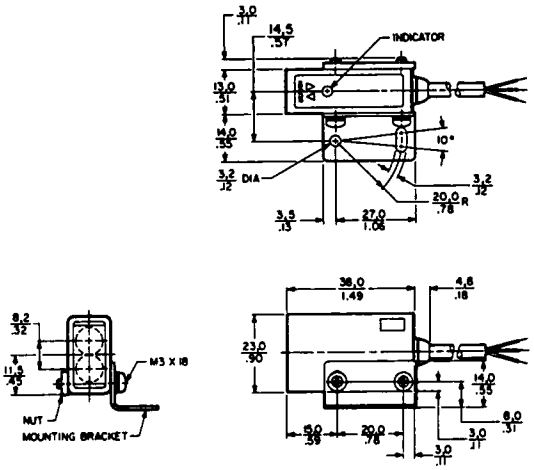

Vertical Mount

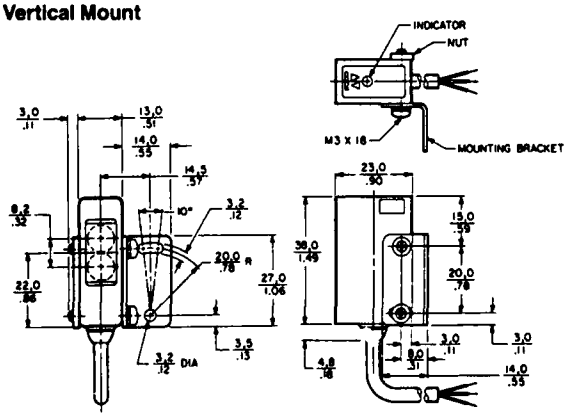

EXCESS GAIN

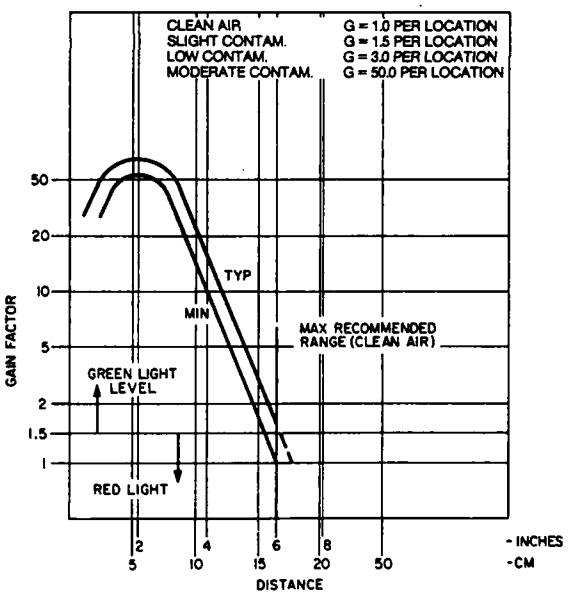

R3 Retroreflective incandescent scanners

FEATURES

- *10-foot retroreflective scan range*
- *Sealing: NEMA 12*
- *Powered from a TRB or G4B Series control base*
- *#15 plug-in incandescent lamp*
- *10,000 hour lamp life at 5.5 VAC and 340 mA*
- *Steel housing*
- *Prewired 8-foot cable*
- *Integral steel mounting bracket*

FOR A COMPLETE CONTROL

Required

- Incandescent scanner — FE-R3T
- Reflector — FE-RR1
- Control base

WIRING/INSTALLATION

Instruction Sheet PK 9012 is included with each control, and is also available upon request.

The FE-R3T is pre-wired with a four conductor color coded cable. Connect:

1. blue and white lamp leads to a lamp supply;
2. red and black leads to the control base;
3. shield wire to ground terminal.

Refer to the instruction sheet included with the control base for its wiring.

Maximum Recommended Scan Distances (Clear Air)

	Reflectors				
	FE-RR1 (3-inch dia. acrylic disc)	**FE-RR2 (1×2-inch tape)**	**FE-RR3 (1-inch dia. acrylic disc)**	**FE-RR4 (5/8-inch dia. acrylic disc)**	**FE-RR5 (1×2 inch high contrast tape)**
R3T	10 ft. (3m)	1 ft. (0,3m)	4 ft. (1,2m)	3 ft. (0,9m)	1.3 ft. (0,39m)
R3T1	Not used with retroreflector. Sharp focus at 6 inches (15,2cm).				
R3AT, R3ABG	Not used with retroreflector. Sharp focus at 1-1/2 inches (3,8cm).				

ORDER GUIDE

Description	Listing
Standard general purpose model; phototransistor sensor.	FE-R3T
Fixed sharp focus* at 6 inches for reflective code reading; phototransistor sensor.	FE-R3T1
Fixed sharp focus* at 1-1/2 inches for detecting small objects, or for registration control; phototransistor sensor.	FE-R3AT
Fixed sharp focus* at 1-1/2 inches for registration control with red/orange/brown registration marks; cadmium sulphide photocell sensor with blue-green filter.	FE-R3ABG

*Limited operating range either side of focal point

MOUNTING DIMENSIONS

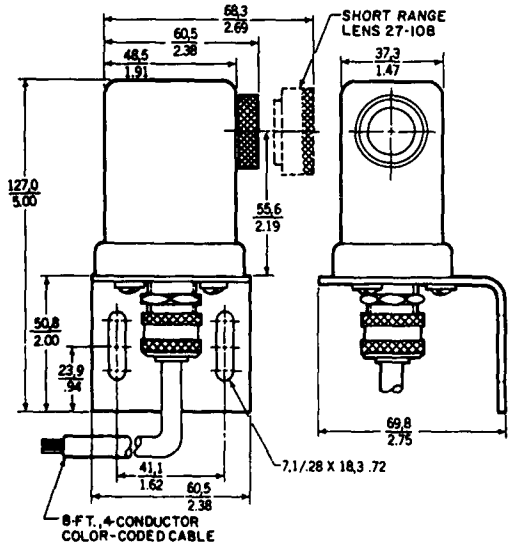

CERTIFICATION OF TECHNICAL DATA CONFORMITY

The Contractor, Vatell Corporation, hereby certifies that, to the best of its knowledge and belief, the technical data delivered herewith under Contract No. F33615-87-C-2801 is complete, accurate, and complies with all requirements of the contract.

1 Mar 1988
Date

Lawrence W. Langley, President

ABSTRACT

Turbomachinery blade clearance and time of arrival sensors based on the Vatell eddy current principle, and suitable for operation at temperatures up to 200°C, were designed, built and tested on the first fan stage of a JT15-D. The sensors produced robust, low noise signals whose general shape is virtually independent of speed, and whose amplitudes are related to speed and clearance. The signals of individual blades were readily resolved and identified. A model equation which predicts sensor signal amplitude, given values of clearance and speed, was developed, and coefficients derived to fit the experimental data. The engine was equipped with an optical once/revolution sensor.